BioPEGylation of Polyhydroxybutyrate (PHB) Promotes Nerve Cell Health and Migration.

ARTICLE *in* BIOMACROMOLECULES · JANUARY 2014

Impact Factor: 5.75 · DOI: 10.1021/bm401572a · Source: PubMed

6 AUTHORS, INCLUDING:

Rodman T. H. Chan
University of New South Wales
5 PUBLICATIONS **34** CITATIONS
SEE PROFILE

Helder Marcal
University of New South Wales
29 PUBLICATIONS **252** CITATIONS
SEE PROFILE

Terry Lee
University of New South Wales
2 PUBLICATIONS **7** CITATIONS
SEE PROFILE

Leslie John Ray Foster
University of New South Wales
80 PUBLICATIONS **1,088** CITATIONS
SEE PROFILE

Article

pubs.acs.org/Biomac

BioPEGylation of Polyhydroxybutyrate Promotes Nerve Cell Health and Migration

Rodman T. H. Chan,[†] Robert A. Russell,[†,‡] Helder Marçal,[†] Terry H. Lee,[§] Peter J. Holden,[‡] and L. John R. Foster*[,†]

[†]Bio/Polymer Research Group, Centre for Advanced Macromolecular Design, School of Biotechnology and Biomolecular Science, and [§]Infection and Inflammation Research Centre, School of Medical Sciences, University of New South Wales, Sydney, New South Wales, Australia

[‡]Australian Nuclear Science and Technology Organisation, Lucas Heights, New South Wales, Australia

ABSTRACT: This study reports on the superior suitability of Polyhydroxybutyrate-polyethylene glycol hybrid polymers biosynthesised by *Cupriavidus necator* over PHB as biomaterials for tissue engineering. Incorporation of PEG106 (DEG) during PHB biosynthesis reduced crystallinity, molecular weight, and hydrophobicity while improving mechanical properties. In vitro olfactory ensheathing cell (OEC) proliferation was enhanced by cultivation on PHB-*b*-DEG films. Cultivation on PHB and PHB-*b*-DEG films showed no cytotoxic responses and cell viability and membrane integrity was sustained. PHB-*b*-DEG films promoted OECs entering into the DNA replication (S) phase and mitotic (G2-M) phase during the cell growth cycle and apoptosis was low. This study also confirmed an association between the level of neurite-outgrowth inhibitory protein (Nogo) and receptor pair Ig-like receptor B (PirB) expression and cell proliferation, both being down-regulated in cells grown on hybrid films when compared with PHB and asynchronous growth. Thus, DEG-terminated PHB-based biomaterials have great potential as biological scaffolds supporting nerve repair.

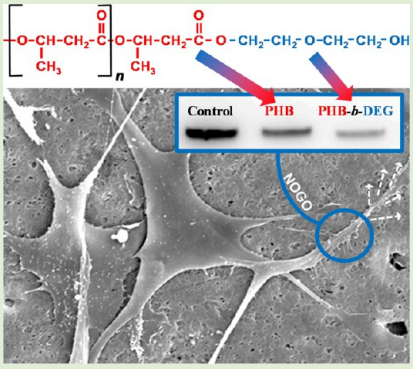

INTRODUCTION

Tissue engineering is dependent upon biomaterials as support scaffolds for cells during in vitro cultivation and subsequent implantation.[1] The development of engineered tissues is reliant on the selection and design of appropriate scaffolding materials. Similarly, tissue responses to implantable medical devices are also reliant upon the device material. Various biopolymers, including polyhydroxybutyrate (PHB), have emerged as potential biomaterial candidates for implantable biomedical devices and tissue engineering scaffolds, supporting cell adhesion, proliferation, and differentiation.[2−4]

Polyhydroxyalkanoates (PHAs) are a family of biopolyesters produced intracellularly in a wide variety of microorganisms and serve as a carbon and energy storage function.[5] Currently, approximately 150 different hydroxyalkanoate monomers have been identified.[6] PHB is the most studied member of the PHA family, its monomer hydroxybutyric acid (3-HBA) is chemically identical to mammalian HBA produced as one of the ketone bodies during prolonged starvation and under diabetic conditions, and is recognized by mammalian enzymes.[7] In addition, there is evidence to suggest that 3-HBA supports cell growth by preventing apoptosis.[8,9] PHB is approved by the Food and Drug Administration (FDA) in the U.S.A. and regulatory bodies in a number of other countries for medical applications.[10] Since its commercial debut in the 1950s, PHB and its composites have been explored for potential applications in a variety of biomedical devices from sutures and bone plates to vein valves, various wound dressings, and tissue scaffolds (for a detailed review see ref 11).

Tabesh et al. recently reported that PHB implants seeded with Schwann cells showed promise in promoting nerve regeneration in the spinal cord.[12] However, there are a number of disadvantages to using Schwann cells, including their interaction with astrocytes and sampling problems.[13] In contrast, olfactory ensheathing cells (OECs) are a type of glial cell vital in promoting the regeneration of nascent neurons in the olfactory system.[14] They can be easily collected with minimal invasiveness from adults and show no interaction with astrocytes. Furthermore, OECs are the only type of cell that continuously ensheath axons from the peripheral to central nervous system (PNS and CNS) respectively.[15] In addition, neurite outgrowth inhibitory protein (Nogo-66) and its receptor pair Ig-like receptor B (PirB) have been expressed from OECs and are known to inhibit neurite outgrowth and axon regeneration.[16,17] Nogo-66 is a 66 amino acid region common to Nogo-A, -B, and -C and is the potent domain that inhibits cell migration.[51] PirB is a high-affinity receptor for the Nogo protein and helps control axonal regeneration.[17]

The potential application of PHB for nerve repair and engineering requires two cellular processes to occur con-

Received: October 24, 2013
Revised: November 19, 2013
Published: December 3, 2013

currently. The cells grow and populate the biomaterial scaffold, whereby the cells cycle through growth phases classified as "G0/G1" (resting), "S" (DNA synthesis), "M" (mitosis), and "G2" (gap between S and M). Typically, it is the G0/G1 phase that is shortened when cells move from a nonproliferative to a proliferative state, while the S, G2, and M phases remain relatively constant. Concurrently, cells differentiate into specific lineages and function to fulfill specific functions. Manipulation of cell growth using biomaterial chemistry is therefore of considerable interest in tissue engineering applications. Neurogenesis involves both cell proliferation and differentiation and cells undergo cell cycles.[19] Undifferentiated cells are programmed to progress through the cell cycle, and while mature neurons exit and cannot re-enter the cell cycle, Gage has suggested that undifferentiated neural cells can be influenced in tissues such as the olfactory epithelium.[20]

The application of PHB as a biomaterial is limited by its brittle nature and relatively lengthy degradation time in vivo.[21] There are numerous studies investigating the manipulation of PHB properties through copolymerising and blending for biomaterial applications.[22,23] Poly(ethylene glycol) (PEG) groups with molecular weights below 600 KDa can act as chain terminating agents during bioprocessing of PHAs resulting in the biosynthesis of natural−synthetic hybrids, that is, "bioPEGylation".[24] Furthermore, during PEG modulated bioprocessing the molecular weight and monomeric composition of the PHAs can be controlled. While a number of reports in this field have focused on the PEG modulated control of PHA bioprocessing, there have been only a few studies on PHA-*b*-PEG hybrids as biomaterials (for detailed review, see ref 25).

Manipulation of PHB material and biological properties through bioPEGylation could provide a more flexible biomaterial to promote regenerative capacity in neurons for tissue engineering applications.[26] Diethylene glycol (DEG as PEG106) is biocompatible with both blood and tissue and is also FDA approved.[27] Thus, we propose that bioPEGylation of hydrophobic PHB using DEG will introduce a hydrophilic component to this hydrophobic biomaterial supporting improvement of its material properties as well as promoting biocompatibility without compromising its FDA status.[28] Furthermore, we compare the response of OECs to films of PHB and its bioPEGylated hybrid (PHB-*b*-DEG), with a detailed examination of cell cycle and their ability to proliferate and migrate. Thus, this study supports the investigation of bioPEGylated PHB as a potential nerve guide, designed to promote regeneration of neurons in nerve repair in tissue engineering.

MATERIALS AND METHODS

Material and Reagents. Polyhydroxybutyrate (PHB) of natural origin, polyethylene glycol (PEG106), and dimethylformamide (DMF) were purchased from Sigma-Aldrich (Sydney, Australia). Chloroform and dimethyl sulfoxide (DMSO) were purchased from Ajax (Sydney, Australia). *Cupravidus necator* (ATCC 17699) was used to produce PHB and PHB-*b*-DEG. Olfactory ensheathing cells (OECs) were routinely cultured in Dulbecco's Modified Eagle's Medium (DMEM/F12), supplemented with 10% fetal bovine serum (FBS), purchased from Lonza (Portsmouth, NH, U.S.A.).

Penicillin and streptomycin antibiotics were obtained from Gibco-Invitrogen (Sydney, Australia). Trypsin and the cell arresting agents aphidicolin and nocodazole were purchased from Sigma Aldrich (St. Louis, U.S.A., and Sydney, Australia). The Cell Titer 96 Aqueous One Cell proliferation assay and in vitro lactic dehydrogenase based toxicology kits were purchased from Promega (Madison, WI, U.S.A.) and Sigma Aldrich, respectively (Wisconsin, U.S.A.). All chemicals were of analytical grade, with a minimum 98% purity.

Biopolymer Production. PHB and its bioPEGylated hybrid were produced through bioprocessing using *Cupravidus necator* (ATCC 17699) in a 15 L bioreactor (Applikon Biotechnology, Netherlands) with a working volume of 10 L using a modification of the method by Ashby et al.[24] Briefly, cells were grown in minimal salt medium with glucose (total of 10 g/L) at 30 °C, pH 6, and 30% dissolved oxygen tension (DOT) for 48 h. Biomass was subsequently harvested by centrifugation (6000 *g*, 30 °C, 30 min), the supernatant was discarded, and the cell pellet resuspended in nitrogen-free minimal salt medium with 20 g/L glucose and 2% v/v DEG before incubating as before for a further 24 h. Biomass was then harvested by centrifugation (8000 *g*, 4 °C, 30 min), washed with reverse osmosis (RO) water and lyophilized for 24 h. Polymer extraction into chloroform and purification through cycles (×3) of precipitation in cold methanol were carried out as per Ashby et al. this also removed residual DEG.[24] The pure polymer was dried under vacuum at 25 °C.

Polymer compositions and bioPEGylation were confirmed using GC and NMR.[29] Samples of PHB purchased from Sigma and bioprocessed PHB and PHB-*b*-DEG prepared were dissolved in chloroform (2% w/v) and fabricated into thin films by casting into clean, dry, sterile glass Petri dishes, dried by standing in a clean biosafety cabinet (12 h, 22 °C), then in a vacuum desiccator (48 h, 40 °C) to remove any residual solvent residues, before returning to the biosafety cabinet to stand for a further 48 h (22 °C) until their weights had atmospherically equilibrated. The films were then aged for a further three weeks to enable their crystallinity to reach equilibrium. Film thicknesses were measured using a digital micrometer (Starrett, 796XFL-1, U.S.A.). Ten locations from the edges and centers of each film were randomly selected and their means determined (n = 10).

Immediately prior to degradation and biocompatibility testing, films were sterilized using γ-irradiation (20 min, 0.564 kGy/h).

Polymer Characterization: Molecular Weight. Molecular masses of PHB and PHB-*b*-DEG were determined by GPC (Varian, PL-GPC 50 Plus, U.S.A.). A PL gel column (5 μm, 2× mixed-C, 300 × 7 mm) was used at 30 °C with a refractive index detector with chloroform as eluent (1 mL/min). Polymer samples were dissolved in chloroform (10 mg/mL) and then filtered using a ministart RC 15 filter before injection. The GPC was calibrated with a series of polystyrene standards (American Polymer, Standard Corporation, U.S.A.) processing low polydispersity (<1.1).

Film Characterization: Thermal Properties. Thermal properties were investigated using a DSC-1 Star^e system (Mettler Toledo, U.S.A.). Samples (5 mg) were sealed in pans and heated at 10 °C/min from 25 to 220 °C to obtain the melting temperature (T_m) and enthalpy of fusion (ΔH_f). Samples were then cooled at the same rate from 220 to −50 °C before reheating from −50 to 220 °C to obtain glass transition temperatures (T_g). The polymer phase crystallinity (PHB-X_c) was calculated using eq 1.[30]

$$\text{PHB} - X_c = \Delta H_f / \Delta H^\circ_f \times 100 \quad (1)$$

where ΔH°_f is the enthalpy of fusion for PHB (146 J g^{1-}).[30] Means of at least three samples were determined (n = 3).

Film Characterization: Crystallinity. X-ray diffraction patterns of the biopolymer films were acquired using a Philips X'pert Material Research Diffraction (MRD) system (Amsterdam, Netherlands). Film samples (20 × 20 mm) were secured on glass slides and aligned with 2θ, z-axis, and omega scans (scattering angle range 2θ = 10−30°, scan step size = 0.02° continuous). A radiation wavelength of 1.5406 Å (Cu Kα) was used to generate a power of 45 kV and tube current of 40 mA. Crystallinity was calculated from the patterns using eq 2.

$$\text{crystallinity}(\%) = [\text{Fc}/(\text{Fc} + \text{Fa})] \times 100\% \quad (2)$$

where Fc and Fa are the areas of crystal (peak) and noncrystal regions (under the curve), respectively.

Film Characterization: Hydrophobicity. Water uptake was measured gravimetrically through water immersion.[31] Preweighed

film samples (40 × 10 mm) were immersed in RO water (37 °C, 5 min) then reweighed after drying with Kimwipes. Water uptakes were calculated accordingly:

$$WU(\%) = (W_2 - W_1)/W_1 \times 100\% \quad (3)$$

were WU is the percentage water uptake and W_1 and W_2 are the film weights before and after immersion, respectively. Means of five samples were determined (n = 5).

Surface hydrophobicity was determined using a sessile drop contact angle meter (KSV cam 200, Finland, CAMD).[32] Water droplets were placed on the biopolymer samples (20 × 20 mm) using a microsyringe and the contact angles determined using KSV software. Means of five readings were determined for each samples (n = 5).

Film Characterization: Material Properties. Material properties were measured using an Instron-5543 tensiometer (Canton, U.S.A.). Film samples (30 × 15 mm) were held between two pneumatic clamps positioned at a distance of 25 mm and pulled apart with a constant cross-head speed of (20 mm/min, 22 °C, 30% rH). The tensile strength and extension at break were calculated using Bluehill computer software (V4.2, Instron, Canton, U.S.A.). Film flexibility of samples (d = 40 mm) was determined through fold endurance, where the repeat number of folds until break or tear were measured as per ISO5626. Means from 10 samples were determined (n = 10).[33]

Ethanol displacement was used to measure the porosity of the biopolymer films.[33] Film samples (50 × 10 mm) were immersed in a measuring cylinder containing a known volume of ethanol (V_1) and the total volume (V_2) recorded after 5 min. The ethanol-impregnated films were then removed and the remaining volume measured (V_3). Means of five samples were determined (n = 5). Film porosities were calculated accordingly:

$$\text{porosity}(\%) = (V_1 - V_3)/(V_2 - V_3) \times 100\% \quad (4)$$

Film Characterization: Surface Roughness. The average surface roughness (R_a) for the samples was calculated using an SRG-4500 surface parameter instrument (Phase II, New Jersey, U.S.A.). The instrument was calibrated using a diamond stylus on a calibration stage and leveled before testing with the samples. A total of five samples for each film were taken and the average R_a values calculated (n = 5).[34]

Film Characterization: Degradability. Preweighed samples of sterilized polymer films (30 × 15 mm) and placed into 2 mL Eppendorf tubes. Samples were incubated with agitation (37 °C, 150 rpm) following the addition of phosphate buffered saline (0.1 M, pH 7.4) with penicillin (100 units/ml), streptomycin (100 μg/mL), and fungizone-amphortericin B (2.5 μg/mL). Samples were periodically removed, filtered, and dried in a desiccator (40 °C, 24 h) before allowing to acclimatize at 22 °C (atmospherically equilibrated weight). Incubation was conducted for 84 days and at constant pH.[35] The procedure was modified from Freier et al.[21] The degradation of the films was expressed as weight loss (%), determined by the eq 5:

$$W(\%) = W_t/W_0 \times 100\% \quad (5)$$

where W is the percentage weight loss and W_0 and W_t are the initial weight and weight after incubation. Means of four samples per time point were determined (n = 4).

Cell Proliferation and Morphology. Adherent OECs were cultivated in sterile T75 tissue flasks containing DMEM medium supplemented with 10% FBS, (37 °C, 5% CO_2) and harvested at 70% confluence.[33] Populations of approximately 4 × 10^4 cells/mL were used to inoculate films samples (13 × 13 mm, 8 replicates) coating glass tissue dishes and incubated (37 °C, 5% CO_2). Controls inoculated in the absence of the polymers were simultaneously conducted. At periodic intervals, samples were rinsed twice with 10 mL of PBS containing 2 mL of trypsin (2.5% v/v) before further incubating for 2 min (37 °C, 5% CO_2). Cell proliferation and viability were calculated using a hemocytometer/automated cell counter and the trypan blue exclusion technique over a period of 10 days.[34] Triplicates per film and per time point were used for each proliferation assay (n = 3 × 8).

OECs attached to polymer films were visualized using SEM as per Ahmed et al.[36] Cells cultivated on the polymer films had their aspirated medium removed and the specimens subsequently rinsed with 1% PBS twice prior to fixing in 0.1 M PBS containing 2.5% glutaraldehyde solution (22 °C, pH 7.4, 4 h). Films were then washed with PBS buffer for 3 cycles (5 min each) and subsequently dehydrated stepwise in a series of ethanol washes (from 30, 50, 70, 80, 90, and 95 to 100%) for 10 min at each concentration. Films in 100% ethanol were critical point dried using liquid CO_2 then mounted on aluminum stubs and sputter coated with gold (2 min, 20 mA, Emitech K550x, Hertfordshire, England). Samples were examined using an Hitachi S3400−N scanning electron microscope (Japan) at 15 kV and 30 mA.

Mitochondrial Activity and Membrane Integrity. OECs were cultured in DMEM-10% FBS medium, harvested by trypsinization, and populations of approximately 3 × 10^3 cells/mL used to inoculate 96-well plates coated with polymer films, cells cultivated in the absence of the biomaterials were used as control. Plates were incubated (37 °C, 5% CO_2, 48 h) and mitochondrial activity and membrane integrity assayed. Mitochondrial function in the OEC populations was assessed using a Cell Titer 96 Aqueous one cell proliferation assay with the addition of 30 μL of MTS (3-(4,5-dimethylthiazol-2-yl)-2,5-diphenyltetrazolium bromide) solution to each well before another 4 h incubation. MTS concentrations were then measured at 490/690 nm using a microtiter plate spectrophotometer (Spectra Max 3400, Molecule Device, U.S.A.).

Leakage of lactate dehydrogenase (LDH) was used to measure membrane integrity in the OEC populations as a consequence of their incubation with the polymer films.[35] At 45 min prior to the incubation end point, 10 μL samples of lysis solution were added to five of the wells and these served as positive controls. After incubation, plates were centrifuged (300 g, 5 min, 22 °C, rH 30%) and 50 μL samples of the supernatants transferred to sterile plates. Samples of LDH mixture (100 μL) were then added to each well before incubating in the dark for 30 min (37 °C, 5% CO_2). LDH analysis was performed at 490/650 nm using the microtiter plate spectrophotometer. Means of five replicates per sample were determined (n = 5).

Cell Cycle and Apoptosis. OECs were cultured in DMEM-10% FBS medium in sterile glass tissue culture dishes coated with the polymer films and grown for 5 days with a working volume of 12 mL. Controls for DNA content were simultaneously conducted including (1) cells without biopolymers, (2) cells in serum-free medium, and cells synchronized for 48 h in medium containing either 1 μg/mL aphidicolin (3) or 2 μM nocodazole (4). During harvesting, cells subjected to the DNA content assay were centrifuged (300 g, 5 min), washed once in PBS, and then resuspended with cell cycle staining buffer at a concentration of 1 × 10^6 cells/mL and incubated on ice (30 min) before analysis using a flow cytometer (Beckman Coulter, Quanta SC MPL, Australia).

Apoptotic indices associated with the externalization of phosphotidylserine (PS) were assayed using an FITC-conjugated Annexin-V apoptosis kit and counterstained with propidium iodide (PI; BD Bioscience, Pharmingen, U.S.A.).[35] Controls for apoptosis used OECs subjected to 2 μM nocodazole for 24 h in the presence of DMEM with 10% FBS, while controls of healthy cells were conducted using the same conditions with the absence of apoptosis inducing agents. Prior to analysis, cells were harvested and washed once in PBS. FITC and PI molecules were visualized using a Becton and Dickinson FACS Calibur Flow Cytometer equipped with a 488 nm laser. Homogenous populations were identified using bivariate forward and side-angle scatter gating, while excluding cellular debris and dead cells. The fluorescence of FITC and PI were visualized using 530/30- and 585/42-bandpass filters, respectively; 10000 events for Annexin-V and 50000 events for DNA content histograms. Photomultiplier (PMT) voltages were attuned to ensure that autofluorescence associated with nonapoptotic samples described a Gaussian distribution within the first two log-decade on univariate histograms (Summit v3.1 software, Cytomation, Fort Collins, CO). PI staining solution contained 0.1% (v/v) Triton X-100, 0.1% (w/v) BSA, 40 μg/mL PI, and 10 μg/mL RNase A in PBS. Cells were extracted through centrifugation (300 g, 5

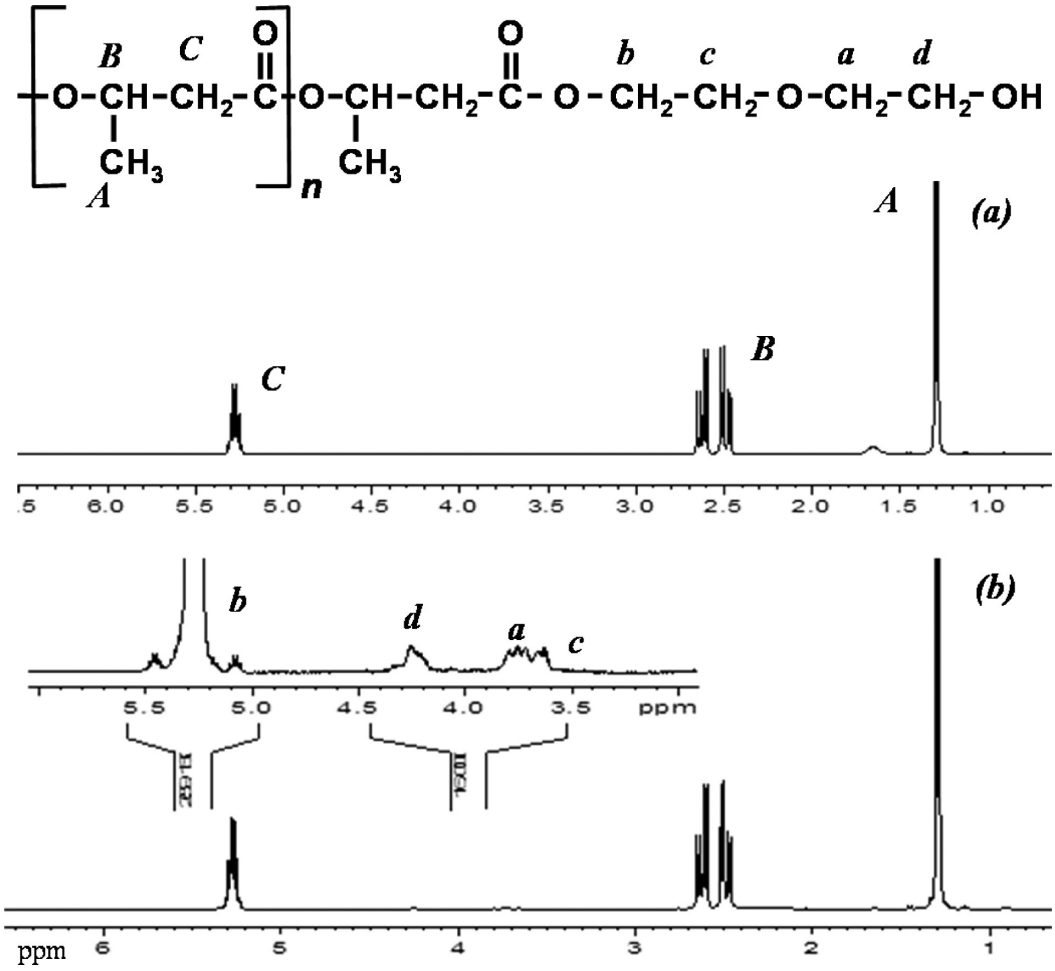

Figure 1. ^{1}H NMR spectra of (a) polyhyroxybutyrate, PHB, and its (b) bioPEGylated hybrid with diethylene glycol, DEG.

min), rinsed once in PBS, and centrifuged again. Cells were then resuspended, transferred to FACS tubes, and incubated in staining solution for 30 min on ice. PI fluorescence intensities were deconvulated using ModFit (Verity Software House, Inc., Topsham, ME) to resolve cell cycle distributions. Cell studies were performed in triplicate and experiments repeated ($n = 3 \times 2$).

Expression of Neurite-Outgrowth Inhibitory Proteins. OECs were cultivated on biopolymer films as described above but with additional samples containing His-Nogo 66 protein (100 nm).[37] Cells were harvested after 3 days, washed twice with PBS, lysed with radioimmunoprecipitation assay buffer (RIPA), and quantified by bicinchoninic acid assay (BCA). Protein samples (10 μg) were loaded in a 10% SDS PAGE gel, transferred to PVDF membrane, and blocked with 5% skimmed milk. The membrane was then probed with anti Nogo-A/B (Imgenex, U.S.A.), anti-PirB (Santa Cruz, U.S.A.), or anti-GAPDH (Abcam, U.S.A.) antibodies and developed with chemiluminescence. The quantity of expressed protein was normalized to glyceraldehyde 3-phosphate dehydrogenase (GAPDH). The images were imported to NIH Image J for quantitative analysis.

Statistical Analysis. All data was statistically evaluated using ANOVA analyses and Bonferroni post-test with a 95% significance level ($p < 0.05$).

RESULTS AND DISCUSSION

Polymer and Film Characterization. Consistent with previous reports, the biopolymer produced through bioprocessing in this study was confirmed as PHB using GC-MS and ^{1}H NMR (Figure 1a).[38] Similarly, DEG modulated cultivation resulted in the end-capping of PHB chains to form a natural-synthetic hybrids of PHB-*b*-DEG (Figure 1b).[24,25] However, in contrast to previous flask culture studies, PHB biosynthesis in a process controlled bioreactor at 10 L scale produced polymer with significantly greater molecular weight of 1143312 g/mol, compared to 522205 g/mol for commercially supplied PHB from Sigma, an increase of 119%. However, the difference in molecular weight number between the two PHB samples was only 18%, reflecting that the PHB produced here had a significantly higher polydispersity index (6.71) compared with 3.62 measured for the Sigma PHB (Table 1). While the polydispersity of bioPEGylated PHB (3.02) was similar to the commercial PHB (3.62), the PEG-modulated bioprocessing significantly reduced the molecular masses of the hybrid. Compared to the PHB from *C. necator*, the bioPEGylated PHB exhibited an 87% decrease in molecular weight (145878) and a 73% decrease in molecular weight number (48326; Table 1).

A standard protocol for film fabrication using 15 mL of polymer solution (2% w/v) and a 90 mm diameter sterile glass Petri dish was applied to produce polymer films with thicknesses ranging from 56 to 85 μm (Table 1). Film thicknesses varied significantly between the polymers, films fabricated from PHB sourced from Sigma had a thickness of 56 $\pm$ 5 μm, while their high molecular weight counterparts from bioprocessed PHB (produced by *C. necator*) were 85 $\pm$ 10 μm. In contrast, PHB-*b*-DEG films were 74 $\pm$ 10 μm. These differences in film thickness may have been caused by variations in crystallization rates and nucleation behavior as well as

dx.doi.org/10.1021/bm401572a | *Biomacromolecules* 2014, 15, 339−349

Table 1. Physiochemical and Material Properties of PHB Films from Sigma and Produced by *C. necator* and PHB-*b*-DEG Films

samples properties	PHB (Sigma)	PHB (*C. necator*)	PHB-*b*-DEG (*C. necator*)
molecular weight (g/mol)	522205	1143312	145878
molecular weight number (g/mol)	144063	170309	48326
polydispersity index	3.62	6.71	3.02
melting point (°C)	179.54 ± 2.67	177.10 ± 1.84	176.87 ± 1.51
glass transition temperature (°C)	0.84 ± 0.08	0.06 ± 0.01	−1.69 ± 0.09
crystallinity, DSC (%)	61.0 ± 2.34	59.0 ± 1.5	44.0 ± 2.1
crystallinity, XRD (%)	70 ± 4	63 ± 5	49 ± 4
film thickness (μm)	56 ± 5	85 ± 10	74 ± 8
film fold endurance (#)	28 ± 2	27 ± 3	32 ± 1
film tensile strength (MPa)	14.5 ± 1.28	18.0 ± 1.39	28.8 ± 3.10
film extension to break (%)	1.8 ± 0.37	2.3 ± 0.51	3.1 ± 0.47
film porosity (%)	58 ± 3	64 ± 2	69 ± 5
water contact angle (°)	90.3 ± 1.7	69.8 ± 1.34	61.2 ± 2.1
water uptake (%)	2.6 ± 0.34	7.4 ± 1.9	17.37 ± 2.67
avg surface roughness (μm)	0.71 ± 0.04	0.51 ± 0.04	0.22 ± 0.04

changes in polymer chain conformation as a consequence of bioPEGylation and their influence on polymer density.[33,39]

X-ray diffraction patterns of the polymer films were consistent with those reported for PHB and were composed of three signature peaks at 14, 17, and 21°, although the intensity of peaks exhibited by the PHB-*b*-DEG film were lower (Figure 2).[40] Quantitative analysis of the XRD spectra showed

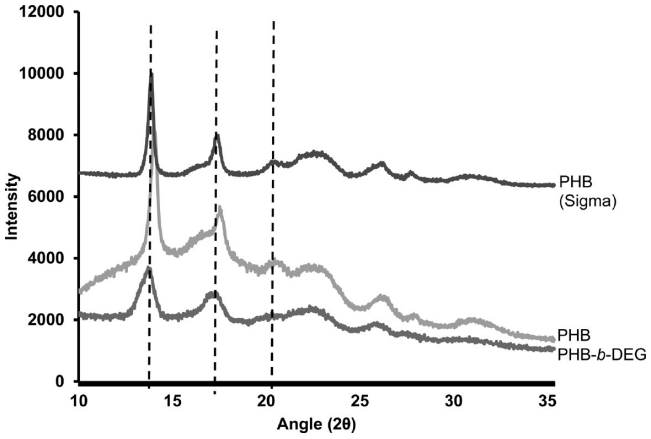

Figure 2. X-ray diffraction patterns of solvent cast films of commercial and bioprocessed PHB and its bioPEGylated hybrid (PHB-*b*-DEG); bioprocessed polymers produced using *C. necator*.

similar crystallinities for the PHB films, 70 ± 4 and 63 ± 5% for PHB from Sigma and *C. necator*, respectively. In contrast, solvent cast films of the hybrid possessed a significantly lower crystallinity, 49 ± 3% ($p < 0.05$, Table 1). DSC analysis supported the XRD data, showing a reduction in crystallinity from 59.0 ± 1.5% for PHB from *C. necator* to 44.0 ± 2.0% for its bioPEGylated hybrid (Table 1). While the melting points for all the polymers showed little variation and remained around 178 °C, the glass transition temperature of PHB-*b*-DEG showed a slight but significant decrease from 0.06 ± 0.01 for PHB to −1.69 ± 0.09 (Table 1). These results suggest that bioPEGylation would not interfere with current commercial thermal processing techniques for PHB.

Molecular weight and crystallinity are important parameters influencing PHA degradation behavior.[41] The relatively high crystallinity of PHB supports a lengthy abiotic degradation under physiological conditions. In the study here, the comparatively higher molecular weight of PHB produced using *C. necator* reduced the initial weight loss, with only 2% lost after 20 days incubation compared to approximately 6% for the PHB from Sigma and 7% for the PHB-*b*-DEG films. However, the degradation profile for films fabricated from commercial PHB displayed a plateau with no significant weight loss between days 20 to 70, suggesting that the initial weight loss may have been due to low molecular weight components within the film, consistent with (Figure 3).[41,42] In contrast,

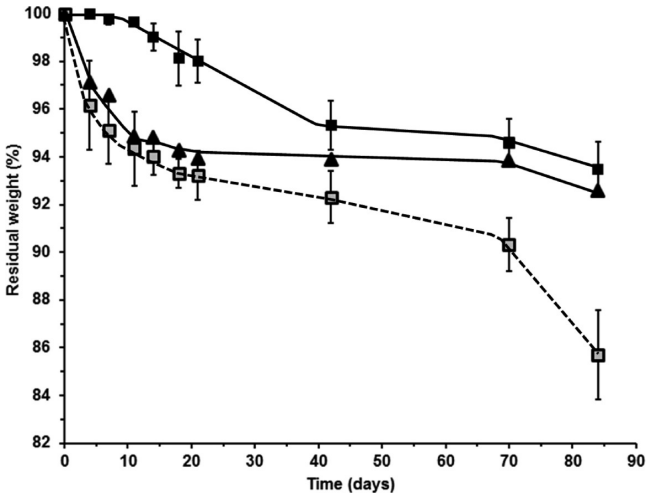

Figure 3. Degradation of solvent cast films under physiological conditions (37 °C, pH 7.4, 150 rpm) as measured through weight loss and expressed as percentages of initial weight; (▲) PHB from Sigma, (■) PHB, and (□) PHB-*b*-DEG hybrid produced through bioprocessing using *C. necator*.

films produced from bioprocessed PHB and PHB-*b*-DEG continued to degrade, after 84 days incubation the PHB films had lost about 7% of their initial weight, while the bioPEGylated films lost 15% (Figure 3). Thus, bioPEGylation promoted PHB degradation under physiological conditions.

Crystallinity is also an important parameter affecting the material properties of polymers.[43] In the study here, the solvent cast films fabricated from commercial and bioprocessed PHB had similar tensile strengths, 14.5 ± 1.28 and 18.0 ± 1.39 MPa, respectively, and similar extension at breaks (1.8 ± 0.37 and 2.3 ± 0.51%), despite the significant differences in their respective molecular weights (Table 1). In contrast, bioPEGylation of PHB significantly improved the material properties, with an approximately 90% increase in tensile strength (28.84 ± 3.10 MPa) and 50% increase in extension at break (3.13 ± 0.47%). Similar results were observed in Foster et al. where bioPEGylated PHA hybrid films produced from *A. latus* were more flexible than their nonhybrid counterparts.[44] Furthermore, the PHB-*b*-DEG films were more flexible with a slight

dx.doi.org/10.1021/bm401572a | *Biomacromolecules* 2014, 15, 339−349

but significantly greater fold endurance (~32 ± 1) when compared to the PHB films (~27 ± 2).

Biocompatibility Studies: Cell Proliferation and Health. OECs were cultivated in the presence of the different PHB-based films and their growths monitored (Figure 4).

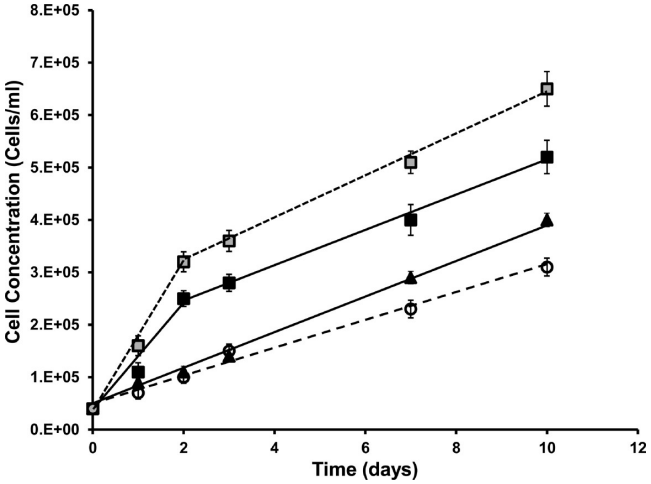

Figure 4. Changes in proliferation of OECs as concentration of cells attached to (○) tissue culture flask, (▲) PHB from Sigma, (■) PHB, and (□) PHB-*b*-DEG hybrid films produced through bioprocessing using *C. necator*. Cells cultured at 37 °C, 5% CO_2 in DMEM + 10% FBS growth media.

There were significant differences in the OEC proliferation profiles between the two types of PHB films. OECs cultivated on films fabricated from commercial PHB exhibited a linear growth rate of approximately 1.5×10^3 cells/mL/h. In contrast, cells grown on its bioprocessed equivalent showed a significant increase within the first 48 h incubation (~4.4×10^3 cells/mL/h) followed by a linear expansion similar to those on the commercial PHB (~1.4×10^3 cells/mL/h, Figure 4). Surface chemistry and morphology can influence cell adhesion and proliferation.[43] In the study here, the higher molecular weight of the bioprocessed PHB resulted in a significantly lower crystallinity, surface roughness, and thicker film compared to its commercial counterpart, this subsequently resulted in an increase in porosity, from 58 ± 3 to 64 ± 2% (Table 1). This slight but significant change in porosity also promoted a more hydrophilic surface, as determined by water contact angles which decreased substantially from 90.3 ± 1.72 to 69.8 ± 1.34° (Table 1). Similarly a significant increase in water uptake was also measured, from 2.6 ± 0.3% for films of commercial PHB to 7.4 ± 1.9% for their bioprocessed counterparts (Table 1). When the hydrophilic component of the DEG was introduced to the PHB through bioPEGylation, these changes in porosity (69 ± 5%), surface roughness (0.22 ± 0.04), water contact angle (61.2 ± 2.1°), and uptake (17.37 ± 2.67%) were emphasized even further. Consequently, OECs cultivated on the PHB-*b*-DEG films showed a similar profile to those grown on the bioprocessed PHB, but with significantly greater rates, about 5.8×10^3 cells/mL/h, followed by a linear rate of about 1.7×10^3 cells/mL/h ($P < 0.05$, $n = 3$; Figure 4). NMR analysis of the PHB-based films post cell studies showed no relative depletion of the DEG moiety, confirming bioPEGylation.

Cells cultivated on the different PHB based films appeared healthy with good spreading and a number of filopodial extensions (Figure 5). These actin-containing filopodiae are considered to be structurally important for cellular mobility and guidance.[35] Further evidence of cell health was obtained through analysis of the OEC mitochondrial activity and

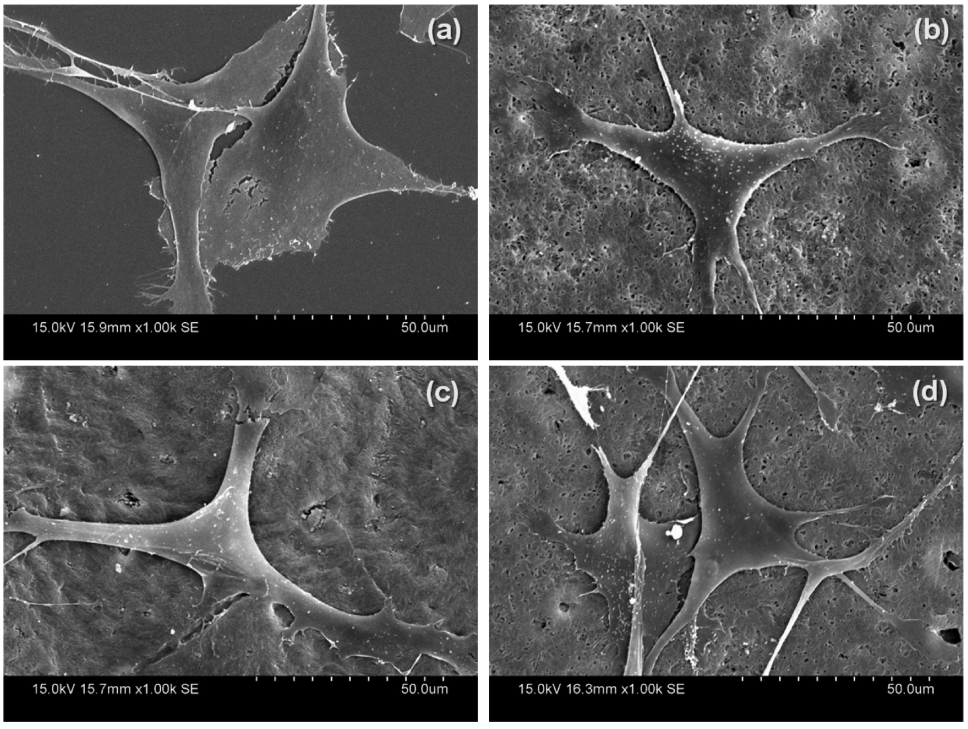

Figure 5. Scanning electron micrographs illustrating morphology of OECs attached to various surfaces after 24 h of cultivation (37 °C, 5% CO_2 in DMEM +10% FBS growth media): (a) Tissue culture flask and solvent cast films of (b) PHB from Sigma and (c) PHB and (d) PHB-*b*-DEG hybrid produced through bioprocessing using *C. necator*; (Magn. x1k, bar = 50 μm).

dx.doi.org/10.1021/bm401572a | *Biomacromolecules* 2014, 15, 339−349

membrane integrity. The mitochondrial activity of OECs was determined by MTS assay which reduces the yellow MTS tetrazolium salt substrate into a purple formazan compound and can also be used as an indicator of cell viability.[45] In the study here, MTS concentrations relative to the asynchronous growth control (assigned 100%) were significantly reduced for OECs cultivated on films cast using commercial PHB (80.3 ± 5.0%). However, consistent with the proliferation studies, the concentrations from OECs grown on the higher molecular weight PHB films was significantly greater (90.8 ± 4.6%), emphasizing the importance of surface morphology and chemistry in dictating cellular biocompatibility. Consistent with this trend, OECs grown on the hybrid showed no significant change (95.7 ± 4.9%) compared to those exhibiting asynchronous growth on tissue supporting polystyrene (Figure 6a). This suggests that the OECs were comparatively more viable with the PHB-*b*-DEG hybrid films than the PHB and this is supported by their comparatively higher cell proliferation.

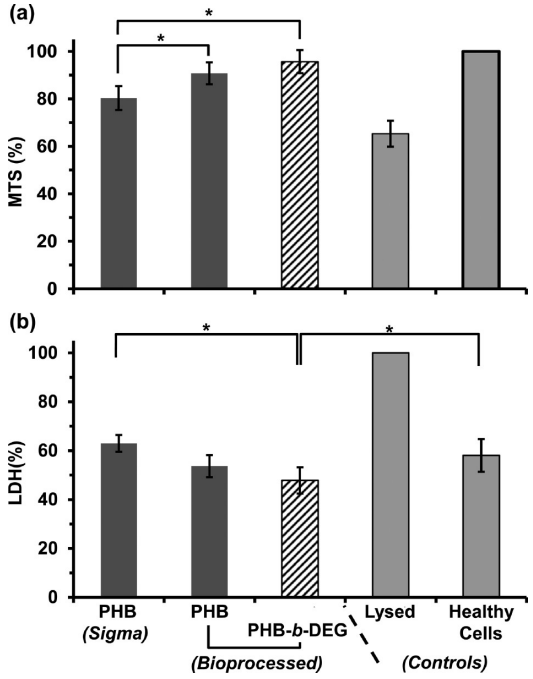

Figure 6. Changes in cell health relative for OECs cultivated (37 °C, 5% CO_2 in DMEM + 10% FBS growth media) in the presence of solvent cast PHA-based films expressed a relative to cells exhibiting asynchronous growth: (a) MTS and (b) LDH concentrations (*P < 0.05 significance, n = 10).

Under stressful and toxic conditions, cell membranes become permeable and release lactate dehydrogenase (LDH); thus, LDH release can also be used as a measure of cellular cytotoxicity through membrane integrity.[46] In the study here, cells undergoing asynchronous growth exhibited an LDH concentration of 58.1 ± 6.7%, which was significantly lower than the lysed cells that served as a control and assigned 100%. OECs cultivated on commercial PHB films released a similar LDH concentration to those in asynchronous growth (Figure 6b). Consistent with the proliferation data, films of PHB from *C. necator* showed a slight but significant decrease in the concentration of LDH released, 53.7 ± 4.6%, this trend continued for OECs cultivate on PHB-*b*-DEG films, 47.85 ± 5.3% (Figure 6b). Thus, the membrane integrity of OECs cultivated on the biopolymers was maintained and promoted on the bioPEGylated hybrid.

Apoptosis was explored in more depth using an Annexin V assay, which quantifies the proportions of a cell population demonstrating externalization of phosphatidylserine (PS), a plasma membrane protein that is externalized once apoptosis has occurred and consequently detected on the cell surface by staining with Annexin V FTIC/PI.[47] Figure 6 shows that OECs cultured in 10% FBS displayed spontaneous apoptosis and necrosis, 8.0 ± 1.3 and 5.2 ± 1.2%, respectively. In contrast, there was a significant increase in apoptosis (51.55 ± 1.78%) and the investigation of necrosis demonstrated 45.40 ± 1.65% when cells were cultured in 2 μM of the arresting agent nocodazole for 24 h. There were no significant differences in the cell populations showing apoptosis and necrosis when cultivated on films of PHB purchased from Sigma compared with healthy cells. However, OECs cultivated on films of bioprocessed PHB showed significant increases in apoptosis after 120 h incubation when compared to those exhibiting asynchronous growth, while the percentage of necrotic cells were similar. Consistent with proliferation and other cell health data, the percentage of OECs exhibiting apoptosis or necrosis when cultivated on PHB-*b*-DEG were significantly reduced, 10.6 ± 1.9 and 3.0 ± 0.5%, respectively, when compared to those cultivated on their PHB counterparts (Figure 7).

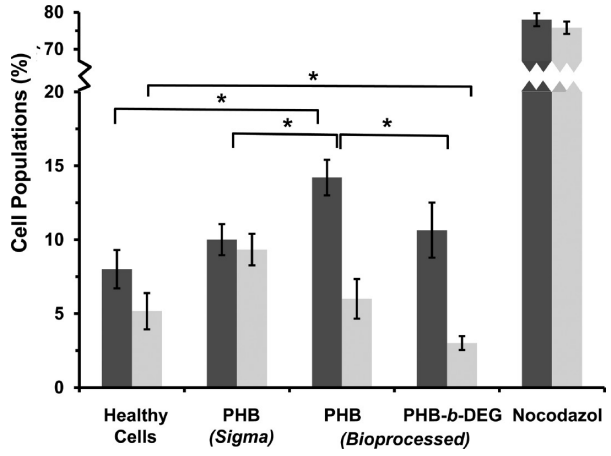

Figure 7. Percentages of apoptotic (dark gray) and necrotic (light gray) OECs when cultivated (37 °C, 5% CO_2 in DMEM +10% FBS growth media) during asynchronous growth and in the presence of solvent cast PHA-based films.

Furthermore, while the populations of OECs displaying apoptosis when cultivated on the PHB-*b*-DEG films were statistically similar to those exhibiting asynchronous growth, the percentage of necrotic cells were significantly reduced: 3.0 ± 0.5% compared to 5.2 ± 0.5% (Figure 7). For all the biomaterials studied here, the apoptotic and necrotic cell populations were maintained below 15%, affirming their biocompatibility.

Biocompatibility Studies: Cell Cycle. While PHB biocompatibility with various cell lines has been studied, reports of its influence on cell health, as determined through cell cycle progression, are limited to Ahmed et al.[37] Similarly, while we have previously reported that bioPEGylation of PHO promoted the progression of myoblastic cell cycle, there are no studies reporting the influence of PHB bioPEGylation on the health of any cell lines.[33,35] In the study here, qualitative

analysis of the FACS histograms in Figure 8 clearly shows that the OECs cycled through the G0/G1, S, and G2-M phases;

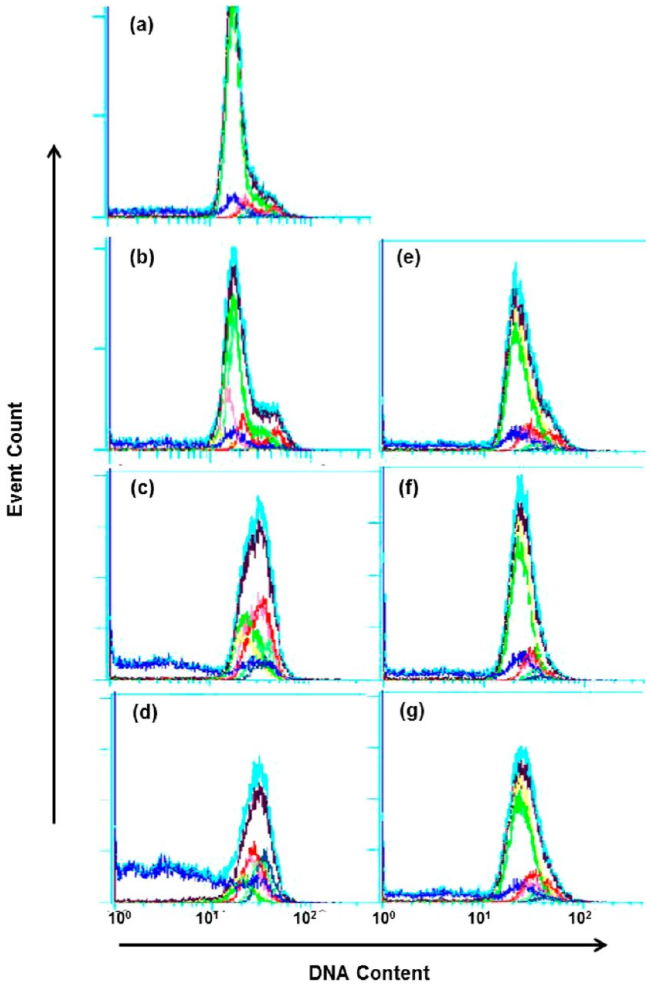

Figure 8. Histograms of OEC populations of exhibiting G0/G1, S, and G2-M growth phases when cultivated (37 °C, 5% CO_2 in DMEM +10% FBS growth media) with/without solvent cast PHA-based films: positive controls for (a) G0/G1 phase through serum deprivation, (b) S phase through addition of aphidicolin, (c) G2/M phase through addition of nocodazole, (d) asynchronous growth, (e) PHB from Sigma, (f) PHB, and (g) PHB-*b*-DEG produced through bioprocessing using *C. necator*.

serum deprivation maintained the cells in the G0/G1 quiescent phase, while positive controls using aphidicolin and nocodazole were used to induce cells to enter the S (DNA synthesis) and G2/M (gap and mitosis) phases, respectively. In comparison to these controls, OECs exhibiting asynchronous growth and those cultivated on the PHB and PHB-*b*-DEG films showed noticeable changes (Figure 8). As anticipated, quantitative analysis of the FACS data revealed significant differences in cell populations when cultivated in the presence of the aphidicolin and nocodazole ($p < 0.01$) compared to those for the control without biomaterials. Similarly, cell populations cultivated with serum deprivation were also comparatively different, verifying the validity of the cultivation protocol (Figure 9).

OECs cultivated on films of PHB sourced from Sigma showed no significant variations in their cell cycle compared to those showing asynchronous growth, consistent with the study by Ahmed et al.[37] In contrast, OECs grown on the higher

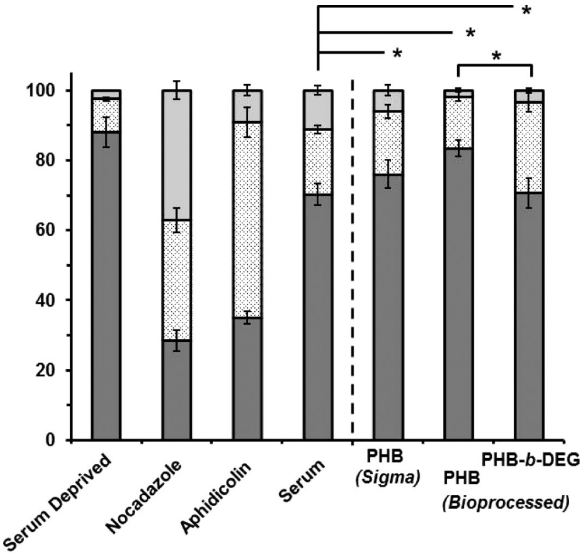

Figure 9. Cell cycle analysis of OEC populations of exhibiting G0/G1 (dark gray), S (patterned), and G2-M (light gray) growth phases when cultivated (37 °C, 5% CO_2 in DMEM +10% FBS growth media) with/without solvent cast PHA-based films; positive controls for G0/G1 phase through serum deprivation, S and G2/M phases through addition of aphidicolin and nocodazole respectively. Summary of DNA content relative to the cell populations determined from data in Figure 7 expressed as percentages of total populations. (*$P < 0.05$ significance, $n = 10$.)

molecular weight PHB films showed a significantly greater population in the quiescent or "resting" phase (G0/G1), 83.5 ± 2.3 compared to 70.3 ± 3.2% for OECs exhibiting asynchronous growth; accompanied by a significant reduction in cells in the G2-M phase, 1.8 ± 0.5% compared to 11.2 ± 1.3% ($p < 0.05$, Figure 8). PHB bioPEGylation promoted a shift in the cell cycle compared to OECs exhibiting asynchronous growth, with a reduction from 11.2 ± 1.3% in the G2-M phase to 3.3 ± 0.7% and a concomitant rise in the S phase, from 18.5 ± 1.2 to 26.0 ± 2.8% (Figure 9). Thus, while the high molecular weight PHB caused a significant shift toward the resting phase (G0/G1), its bioPEGylated counterpart stimulated the cells to the synthesis phase (S), an increase of 12% compared to cells in asynchronous growth ($p < 0.05$). It appears, therefore, that PHB-*b*-DEG stimulated DNA replication and cell division.

Surface chemistry and morphology are known to influence cell attachment and proliferation. In the study here, the average surface roughness (R_a) for the PHB-*b*-DEG films (0.22 ± 0.04 μm) was significantly lower than those of PHB sourced from Sigma and produced from *C. necator* (0.71 ± 0.04 and 0.51 ± 0.04 μm, respectively). Furthermore, the bioPEGylated PHB films possessed significant differences in their hydrophobicity compared to the PHB films. Thus, PHB-*b*-DEG films possessed a water uptake and contact angle of 17.37 ± 2.67% and 61.20 ± 2.1°, respectively, while the PHB films showed 7.40 ± 1.9% and 69.80 ± 1.3°, respectively (Table 1). Therefore, the changes in water uptake, surface hydrophobicity, and roughness through bioPEGylation may have been responsible, in part, for the changes in cell cycle progression. In addition, Saad et al. demonstrated that the monomeric degradation product of PHB can promote cellular activity, thus, the presence of low concentrations of 3-HBA may have stimulated cell proliferation and activity.[2,9]

dx.doi.org/10.1021/bm401572a | *Biomacromolecules* 2014, 15, 339−349

Biocompatibility Studies: OEC Migration. Nogo-66 and its receptor PirB are known to inhibit neurite outgrowth and axon regeneration.[16,17] Nogo is a central nervous system, myelin-associated regulator of neurite outgrowth, its Nogo-66 domain has been found to inhibit axonal extension.[48] Remodelling of axonal regeneration is mainly regulated by Nogo-A, whereas Nogo-B regulates cytoskeletal structures.[49,50] PirB is a high-affinity receptor for the Nogo protein and helps mediate axonal regeneration.[17] The Western blot in Figure 10

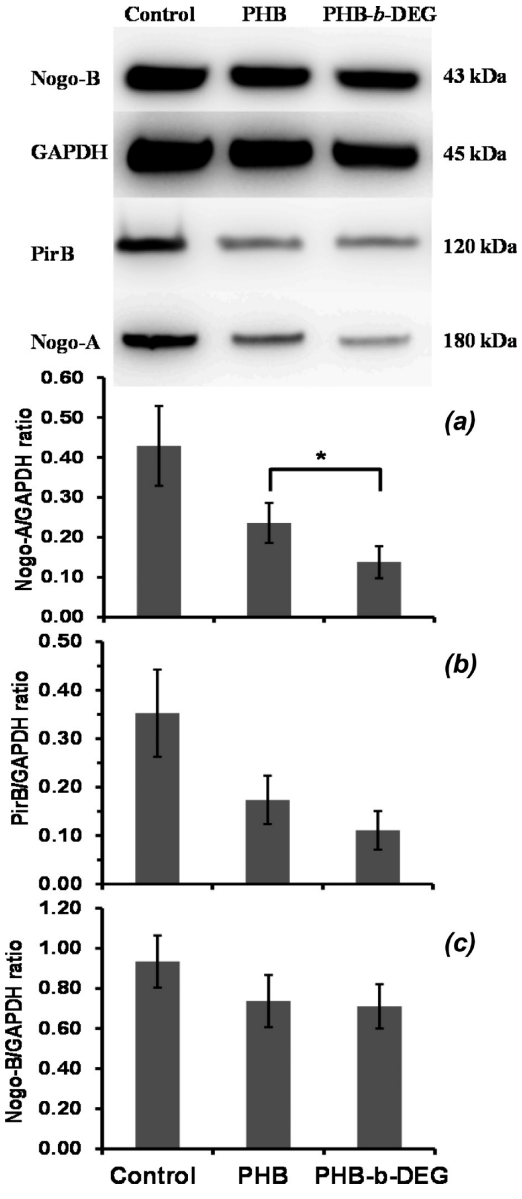

Figure 10. Western blot analysis illustrating the effects of solvent cast films of PHB and PHB-*b*-DEG hybrid, produced through bioprocessing using *C. necator*, on Nogo-A, PirB, and Nogo-B expression by OECs; graphs of protein intensity ratios for (a) Nogo A, (b) PirB, and (c) Nogo B relative to GAPDH.

shows an apparent decrease in the expression of Nogo-A and PirB by the OECs cultured in the presence of the solvent cast PHB and PHB-*b*-DEG films when compared to cells cultured in the absence of biomaterials, exhibiting asynchronous growth. In contrast, there appeared no significant variation in Nogo-B expression. Figure 10a–c shows the quantitative analysis of the Western blot analysis based on protein band intensity. The expression of Nogo-A and PirB was significantly reduced by OECs cultivated in the presence of PHB (0.24 ± 0.05 and 0.17 ± 0.05) and PHB-*b*-DEG films (0.14 ± 0.04 and 0.11 ± 0.04) when compared to cells in asynchronous growth (0.43 ± 0.1 and 0.35 ± 0.09). Similarly, Nogo-B expression showed a slight but significant reduction when cultivated in the presence of the biomaterials.

The data suggests that PHB and PHB-*b*-DEG films reduced the Nogo A/B and PirB expression in OECs cultivated on these films, thereby alleviating the inhibitory regulatory mechanism which promotes cellular proliferation pathways.[51] Karnezis et al. have demonstrated that neurite outgrowth can be restored or maintained by suppressing the Nogo-A activity associated with CNS.[52] Thus, the study here shows that PHB and PHB-*b*-DEG hybrid films affected Nogo-A expression rather than Nogo-B expression in OECs and provides a potential target for axon regeneration therapies. Woodhall et al. have shown that the expression of Nogo-A by OECs was found to be cytoplasmic rather than nuclear or cell surface related.[48]

Nogo-66 is a 66 amino acid region common to Nogo-A, -B, and -C and is the potent domain that inhibits neurite outgrowth and axon regeneration.[18] Woodhall et al. have reported that OECs express the Nogo-66 receptor that binds to Nogo proteins.[48] In the study here, we investigated whether the mechanism of OEC proliferation on PHB and PHB-*b*-DEG films was affected by Nogo-66. Nogo-66 was used as a control and did not have a significant influence compared to the untreated cells (Figure 11). Cell growth in the presence of the

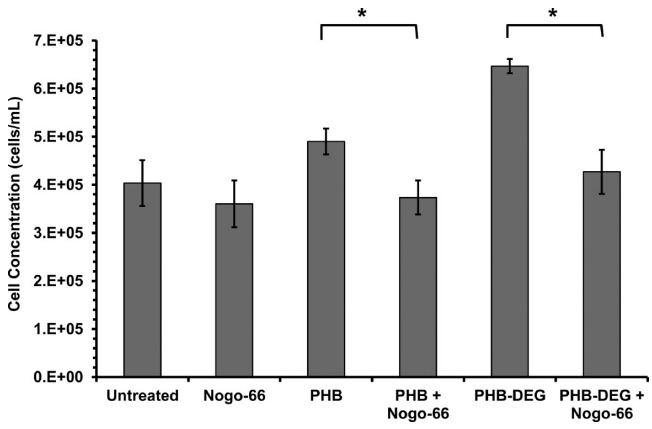

Figure 11. Proliferation of OECs cultivated on solvent cast films of PHB and PHB-*b*-DEG hybrid films and treated with Nogo-66 (100 nM; $*P < 0.05$; $n = 5$).

PHB films was significantly greater than that in the absence of biomaterials, and growth was inhibited by 24% in the presence of Nogo-66. Similarly, OEC growth was promoted by the PHB-*b*-DEG films and was significantly reduced by 34% when treated with Nogo-66.

The influence of Nogo-66 on OEC proliferation may be caused by the inhibitory pathway through either PirB or Nogo receptors.[17,53] Reports suggest Nogo-66 has multiple functions in the process of neuron regeneration. Cao et al. report that OEC migration can be stimulated by a glial cell line-derived neurotrophic factor, while Su et al. have found that Nogo-66 could enhance the adhesion of OECs and inhibit cell migration.[54,55] The results suggest that enhanced proliferation of OECs in the presence of the PHB and PHB-*b*-DEG films

may be associated with a reduced expression of Nogo-A and PirB. The results here show an association between the level of inhibitory myelin protein expression and cell proliferation. Thus, films of PHB-*b*-DEG not only promoted OEC proliferation, but also enhanced cell health while reducing inhibitory myelin protein expression supporting OEC migration.

CONCLUSIONS

PHB and its bioPEGylated hybrid were successfully produced through bioprocessing, and consistent with previous studies, bioPEGylation significantly reduced the PHB molecular weight. Solvent cast films of the bioPEGylated hybrid also exhibited a reduced crystallinity when compared to PHB films, and this may have produced the significant improvements in the material properties. Similarly, the comparative reductions in molecular weight and crystallinity also promoted the hybrids abiotic degradation under physiological conditions, helping to overcome the undesirable lengthy degradation of PHB.

Relative reductions in hydrophobicity, surface roughness and porosity, may have supported enhanced attachment of OECs. The PHB-*b*-DEG films did not trigger any cytotoxic responses by the OECs, which maintained their viability. Furthermore, cell cycle progression cycle was promoted for OECS cultivated in the presence of the hybrid PHB-*b*-DEG films, with a significantly greater proportion of cells in the S-phase. Thus, the novel combination of two FDA approved polymers through bioPEGylation appeared to significantly promote PHB biocompatibility, while helping to reduce its associated disadvantages of brittleness and a lengthy degradation time in the body. Olfactory ensheathing cells have great potential in nerve repair. Their enhanced attachment, proliferation, and health when cultivated with bioPEGylated PHB films correlated with the inhibition of Nogo and PirB proteins expression. The results suggest that bioPEGylated PHB was more likely to support OEC migration, consistent with the increased proliferation and promotion of cell cycle.

The study reported here indicates that bioPEGylation can be effectively used to manipulate the physiochemical, material and biological properties of PHB, enhancing its potential as a biomaterial for biomedical and tissue engineering applications. This current study also demonstrates the potential of bioPEGylated PHB for applications in nerve repair. Furthermore, as both PHB and DEG are FDA approved, progression through the clinical trial pathway could be expedited. The potential of the PHB-*b*-DEG hybrid as an electrospun conduit for the repair of nerve trauma is currently being investigated.

AUTHOR INFORMATION

Corresponding Author

*E-mail: j.foster@unsw.edu.au. Tel.: +61(2)-9385-2054. Fax: +61(2)-9385-1483.

Notes

The authors declare no competing financial interest.

ACKNOWLEDGMENTS

The authors gratefully acknowledge A/Prof. N. Tedla and Dr. K. Bryant from the Immune Regulation Research Group, School of Medical Sciences, University of New South Wales, for supplying Nogo-66 and associated antibodies. The biosynthesized PHB and PHB-*b*-DEG were produced in the National Deuteration Facility at ANSTO, which is partly funded by the Australian Government's National Collaborative Research Infrastructure Strategy.

REFERENCES

(1) Evans, N. D.; Gentleman, E.; Polak, J. M. Scaffolds for stem cells. *Mater. Today* **2006**, *9*, 26−33.

(2) Saad, B.; Neuenschwander, P.; Uhlschmid, G. K.; Suter, U. W. New versatile, elastomeric, degradable polymeric materials for medicine. *Int. J. Biol. Macromol.* **1999**, *25*, 293−301.

(3) Saad, B.; Matter, S.; Ciardelli, G.; Neuenschwander, P.; Suter, U. W.; Uhlschmid, G. K.; Welti, M. Interactions of osteoblasts and macrophages with biodegradable and highly porous polyesterurethane foam and its degradation products. *J. Biomed. Mater. Res.* **1996**, *32*, 355−366.

(4) Wang, L.; Wang, Z. H.; Shen, C. Y.; You, M. L.; Xiao, J. F.; Chen, G. Q. Differentiation of human bone marrow mesenchymal stem cells grown in terpolyesters of 3-hydroxyalkanoates scaffolds into nerve cells. *Biomaterials* **2010**, *31*, 1691−1698.

(5) Numata, K.; Doi, Y. Dual biosyntheses of poly[(*R*)-3-hydroxybutyric acid] and silk protein for the fabrication of biofunctional Bioplastic. *Polym. J.* **2011**, *43*, 642−647.

(6) Vandamme, P.; Coenye, T. Taxonomy of the genus *Cupriavidus*: a tale of lost and found. *Int. J. Syst. Evol. Microbiol.* **2004**, *54*, 2285−2289.

(7) Foster, L. J. R.; Tighe, B. J. Enzymatic assay of hydroxybutyric acid monomer formation in poly *β*-hydroxybutyrate) degradation studies. *Biomaterials* **1995**, *16*, 341−343.

(8) Xiao, X. Q.; Zhao, Y.; Chen, G. Q. The effect of 3-hydroxybutyrate and its derivatives on the growth of glial cells. *Biomaterials* **2007**, *28*, 3608−3616.

(9) Cheng, S.; Chen, G. Q.; Leski, M.; Zou, B.; Wang, Y.; Wu, Q. The effect of D,L-*β*-hydroxybutyric acid on cell death and proliferation in L929 cells. *Biomaterials* **2006**, *27*, 3758−3765.

(10) Zinn, M.; Witholt, B.; Egli, T. Occurrence, synthesis, and medical application of bacterial polyhydroxyalkanoate. *Adv. Drug Delivery Rev.* **2001**, *53*, 5−21.

(11) Chen, G. Q.; Wua, Q. The application of polyhydroxyalkanoates as tissue engineering materials. *Biomaterials* **2005**, *26*, 6565−6578.

(12) Tabesh, H.; Amoabediny, G. H.; Nik, N. S.; Heydari, M.; Yosefifard, M.; Siadat, S. O. R.; Mottaghy, K. The role of biodegradable engineered scaffolds seeded with Schwann cells for spinal cord regeneration. *Neurochem. Int.* **2009**, *54*, 73−83.

(13) Lakatos, A.; Barnett, S. C.; Franklin, R. J. M. Olfactory enshealthing cells induce less host astrocyte response and chondroitin sulphate proteoglycan expression than Schwann cells following transplantation into adult CNS white matter. *Exp. Neurol.* **2003**, *184*, 237−246.

(14) Au, E.; Roskams, A. J. Olfactory ensheathing cells of the lamina propria in vivo and in vitro. *Glia* **2003**, *41*, 224−236.

(15) Barnett, S. C.; Riddell, J. S. Olfactory ensheathing cells (OECs) and the treatment of CNS injury: advantages and possible caveats. *J. Anat. Soc. G. B. Irel.* **2004**, *204*, 57−67.

(16) Gao, Y.; Wang, B.; Xiao, Z. F.; Chen, B.; Han, J.; Wang, X.; Zhang, J.; Gao, S.; Zhao, Y. N.; Dai, J. W. Nogo-66 regulates nanog expression through Stat3 pathway in murine embryonic stem cells. *Stem Cells Dev.* **2010**, *19*, 53−60.

(17) Atwal, J. K.; Gosse, J. P.; Syken, J.; Stawicki, S.; Wu, Y.; Shatz, C.; Lavigne, M. T. PirB is a functional receptor for myelin inhibitors of axonal regeneration. *Science* **2008**, *322*, 967−970.

(18) GrandPré, T.; Nakamura, F.; Vartanian, T.; Strittmatter, S. M. Identification of the Nogo inhibitor of axon regeneration as a Reticulon protein. *Nature* **2000**, *403*, 439−444.

(19) Ohnuma, S.; Harris, W. A. Neurogenesis and the cell cycle. *Neuron* **2003**, *40*, 199−208.

(20) Gage, F. H. Mammalian neural stem cells. *Science* **2000**, *287*, 1433−1438.

(21) Freier, T.; Kunze, C.; Nischan, C.; Kramer, S.; Sternberg, K.; Sab, M.; Hopt, U. T.; Schmitz, K. P. In vitro and in vivo degradation

studies for development of a biodegradable patch based on poly(3-hydroxybutyrate). *Biomaterials* **2002**, 23.
(22) Cheng, G. X.; Cai, Z. J.; Wang, L. Biocompatibility and biodegradation of poly(hydroxybutyrate)/ poly(ethylene glycol) blend films. *J. Biomed. Mater.: Mater. Med.* **2003**, *14*, 1073−1078.
(23) Chen, C.; Cheng, Y. C.; Yu, C. H.; Chan, S. W.; Cheung, M. K.; Yu, P. H. F. In vitro cytotoxicity, hemolysis assay, and biodegradation behavior of biodegradable poly(3-hydroxybutyrate)−poly(ethylene glycol)−poly(3-hydroxybutyrate) nanoparticles as potential drug carriers. *J. Biomed. Mater. Res., Part A* **2008**, *87*, 290−298.
(24) Ashby, R. D.; Shi, F. Y.; Gross, R. A. Use of poly(ethylene glycol) to control the end group structure and molecular weight of poly(3-hydroxybutyrate) formed by *Alcaligenes latus* DSM 1122. *Tetrahedron* **1997**, *53*, 15209−15223.
(25) Lietz, M.; Dreesmann, L.; Hoss, M.; Oberhoffner, S.; Schlosshauer, B. Neuro tissue engineering of glial nerve guides and the impact of different cell types. *Biomaterials* **2006**, *27*, 1425−1436.
(26) Li, X.; Liu, K. L.; Li, J.; Tan, E. P. S.; Chan, L. M.; Lim, C. T.; Goh, S. H. Synthesis, characterization, and morphology studies of biodegradable amphiphilic poly[(*R*)-3-hydroxybutyrate]-*alt*-poly(ethylene glycol) multiblock copolymers. *Biomacromolecules* **2006**, *7*, 3112−3119.
(27) Zanzig, J.; Marimuthu, B.; Werka, J.; Scholz, C. Investigation of the impact of poly(ethylene glycol) - modulation of poly(*β*-hydroxybutyrate) syntheses on cell interactions of the resulting polymers. *J. Bioact. Compat. Polym.* **2003**, *18*, 339−354.
(28) Shi, F. Y.; Ashby, R.; Gross, R. A. Use of poly(ethylene glycol)s to regulate poly(3-hydroxybutyrate) molecular weight during *Alcaligenes eutrophus* cultivations. *Macromolecules* **1996**, *29*, 7753−7758.
(29) Foster, L. J. R.; Sanguanchaipaiwong, V.; Gabelish, C. L.; Hook, J.; Stenzel, M. A natural-synthetic hybrid copolymer of polyhydroxyoctanoate-diethylene glycol: biosynthesis and properties. *Polymer* **2005**, *46*, 6587−6594.
(30) Barham, P. J.; Keller, A.; Otun, E. L. Crystallization and morphology of a bacterial thermoplastic: poly-3-hydroxybutyrate. *J. Mater. Sci.* **1984**, *19*, 2781−2794.
(31) Li, X.; Liu, K. L.; Wang, M.; Wong, S. Y.; Tjiu, W. C.; He, C. B.; Goh, S. H.; Li, J. Improving hydrophilicity, mechanical properties and biocompatibility of poly[(*R*)-3-hydroxybutyrate-co-(*R*)-3-hydroxyvalerate] through blending with poly[(*R*)-3-hydroxybutyrate]-*alt*-poly(ethylene oxide). *Acta Biomater.* **2009**, *5*, 2002−2012.
(32) Townsend, K. J.; Busse, K.; Kressler, J.; Scholz, C. Contact angle, WAXS, and SAXS analysis of poly(*β*-hydroxybutyrate) and poly(ethylene glycol) block copolymers obtained via *Azotobacter vinelandii* UWD. *Biotechnol. Prog.* **2005**, *21*, 959−964.
(33) Foster L. J. R. PEGylation and BioPEGylation of polyhydroxyalkanoates: Synthesis, characterization and applications. *Biopolymers*; Sciyo: Croatia, 2010; Chapter 12, pp 243−256.
(34) Marçal, H.; Wanandy, N. S.; Sanguanchaipaiwong, V.; Woolnough, C. E.; Lauto, A.; Mahler, S. M.; Foster, L. J. R. BioPEGylation of polyhydroxyalkanoates: Influence on properties and satellite-stem cell cycle. *Biomacromolecules* **2008**, *9*, 2719−2726.
(35) Chan, R. T. H.; Marçal, H.; Ahmed, T.; Russell, R. A.; Holden, P. J.; Foster, L. J. R. Poly(ethylene glycol) (PEG) modulated cellular biocompatibility of polyhydroxyalkanoate films. *Polym. Int.* **2013**, *62*, 884−892.
(36) Ahmed, T.; Marçal, H.; Lawless, M.; Wanandy, N. S.; Chiu, A.; Foster, L. J. R. Polyhydroxybutyrate and its copolymer with polyhydroxyvalerate as biomaterials: Influence on progression of stem cell cycle. *Biomacromolecules* **2010**, *11*, 2707−2715.
(37) Chung, R. S.; Woodhouse, A.; Fung, S.; Dickson, T. C.; West, A. K.; Vickers, J. C.; Chuah, M. I. Oflactory enshealthing cells promote neurite sprouting of injured axons in vitro by direct cellular contact and secretion of soluble factors. *Cell. Mol. Life Sci.* **2004**, *61*, 1238−1245.
(38) Sanguanchaipaiwong, V.; Gabelish, C. L.; Hook, J.; Scholz, C.; Foster, L. J. R. Biosynthesis of natural-synthetic hybrid copolymers: polyhydroxyoctanoate-dietyelen glycol. *Biomacromolecules* **2004**, *5*, 643−649.
(39) Xia, C. Y.; Yuan, C. X.; Yuan, C. G. Galanin inhibits the proliferation of glial olfactory ensheathing cells. *Neuropeptides* **2005**, *39*, 453−459.
(40) Shi, F. Y.; Gross, R. A. Microbial polyester synthesis: effects of poly(ethylene glycol) on product composition, repeat unit sequence, and end group structure. *Macromolecules* **1996**, *29*, 10−17.
(41) Chang, L.; Woo, E. M. Crystallization of poly(3-hydroxybutyrate) with stereocomplexed polylactide as biodegradable nucleation agent. *Polym. Eng. Sci.* **2012**, *2012*, 1413−1419.
(42) Hurrell, B. L.; Cameron, R. E. A wide-angle X-ray scattering study of the aging of poly(hydroxybutyrate). *J. Mater. Sci.* **1998**, *33*, 1709−1713.
(43) Bonartsev, A. P.; Boskhomodgiev, A. P.; Iordanskii, A. L.; Bonartseva, G. A.; Rebrov, A. V.; Makhina, T. K.; Myshkina, V. L.; Yakovlev, S. A.; Filatova, E. A.; Ivanov, E. A.; Bagrov, D. V.; Zaikov, G. E. Hydrolytic degradation of poly(3-hydroxybutyrate), polylactide and their derivatives: kinetics, crystallinity, and surface morphology. *Mol. Cryst. Liq. Cryst.* **2012**, *556*, 288−300.
(44) Foster, L. J. R. Biosynthesis, properties and potential of natural-synthetic hybrids of polyhydroxylkanoates and polyehtylene glycols. *Appl. Microbiol. Biotechnol.* **2007**, *75*, 1241−1247.
(45) O'Toole, S. A.; Sheppard, B. L.; McGuinness, E. P. J.; Gleeson, N. C.; Yoneda, M.; Bonnar, J. The MTS assay as an indicator of chemosensitivity/resistance in malignant gynaecological tumours. *Cancer Detect. Prev.* **2003**, *27*, 47−54.
(46) Stolle, L. B.; Hussain, S.; Schlager, J. J.; Hofmann, M. C. In vitro cytotoxicity of nanoparticles in mammalian germline stem cells. *Toxicol. Sci.* **2005**, *88*, 412−419.
(47) Engeland, M. V.; Nieland, L. J. W.; Ramaekers, F. C. S.; Schutte, B.; Reutelingsperger, C. P. M. Annexin V-Affinity assay: A review on an apoptosis detection system based on phosphatidylserine exposure. *Cytometry* **1998**, *31*, 1−9.
(48) Woodhall, E.; West, A. K.; Vickers, J. C.; Chuah, M. I. Olfactory ensheathing cell phenotype following implantation in the lesioned spinal cord. *Cell. Mol. Life Sci.* **2003**, *60*, 2241−2253.
(49) Pot, C.; Simonen, M.; Weinmann, O.; Schnell, L.; Christ, F.; Stoeckle, S.; Berger, P.; Rülicke, T.; Suter, U.; Schwab, M. E. Nogo-A expressed in Schwann cells impairs axonal regeneration after peripheral nerve injury. *J. Cell Biol.* **2002**, *159*, 29−35.
(50) Schanda, K.; Hermann, M.; Stefanova, N.; Gredler, V.; Bandtlow, C.; Reindl, M. Nogo-B is associated with cytoskeletal structures in human monocyte-derived macrophages. *BMC Res. Notes* **2011**, *4*, 1−8.
(51) Mingorance, A.; Solé, M.; Munetón, V.; Martínez, A.; Sampedro, M. N.; Soriano, E.; Río, J. A. Regeneration of lesioned entorhino-hippocampal axons in vitro by combined degradation of inhibitory proteoglycans and blockade of Nogo-66/NgR signaling. *FASEB J.* **2006**, *20*, 491−503.
(52) Karnezis, T.; Mandemakers, W.; McQualter, J. L.; Zheng, B.; Ho, P. P.; Jordan, K. A.; Murray, B. M.; Barres, B.; Lavigne, M. T.; Bernard, C. C. A. The neurite outgrowth inhibitor Nogo A is involved in autoimmune-mediated demyelination. *Nat. Neurosci.* **2004**, *7*, 736−744.
(53) Fournier, A. E.; GrandPre, T.; Strittmatter, S. M. Identification of a receptor mediating Nogo-66 inhibition of axonal regeneration. *Nature* **2001**, *409*, 341−346.
(54) Cao, L.; Su, Z.; Zhou, Q.; LV, B. L.; Liu, X. J.; Jiao, L.; Li, Z. H.; Zhu, Y. L.; Huang, Z. H.; Huang, A. J.; He, C. Glial cell line-derived neurotrophic factor promotes olfactory ensheathing cells migration. *Glia* **2006**, *54*, 536−544.
(55) Su, Z.; Cao, L.; Zhu, Y. L.; Liu, X. J.; Huang, Z. H.; Huang, A. J.; He, C. Nogo enhances the adhesion of olfactory ensheathing cells and inhibits their migration. *J. Cell Sci.* **2007**, *120*, 1877−1887.